

Discrete and Extended Supersandwich Structures Based on Weak Interactions between Phosphorus and Mercury**

Martin Fleischmann, Claudia Heindl, Michael Seidl, Gábor Balázs, Alexander V. Virovets, Eugenia V. Peresyphkina, Mitsukimi Tsunoda, François P. Gabbaï, and Manfred Scheer*

Dedicated to Professor Dieter Fenske on the occasion of his 70th birthday

Supramolecular chemistry based on weak interactions is becoming increasingly important relative to conventional molecular chemistry based on covalent bonds.^[1] In particular, the interaction of planar electron-deficient molecules has developed into a rich area of research with ongoing applications in anion recognition,^[2] molecular machines,^[3] or light-emitting materials.^[4] Prototypical examples of such electron-deficient molecules include pyridinium cations,^[3] electron-deficient aromatic compounds,^[2] and also, in some case, organometallic derivatives, such as trimeric (perfluoro-*o*-phenylene)mercury ($[(o-C_6F_4Hg)_3]$, **1**).^[4,5] The latter is a planar trinuclear mercury derivative that readily engages electron-rich aromatic hydrocarbons into weak donor–acceptor interactions, leading to the formation of extended binary adducts.^[5b,6] Remarkably, this molecule can also interact with aromatic ligands bound to transition-metal ions. This is for example the case of the simple metallocenes $[Cp_2Fe]$ and $[Cp_2Ni]$, which interact with **1** to form double-sandwich structures with the double-decker organometallic species trapped between two molecules of **1** (arrangement **I** in Figure 1).^[7] Inspired by these unusual architectures, we have now decided to study how **1** would behave towards triple-decker complexes containing a polyphosphorus middle deck. Herein, we report the results of such an investigation with the triple-decker complexes of the $[(Cp^R Mo)_2(\eta^6-P_6)]$ family ($Cp^R = Cp, Cp^*$). As an added incentive for these studies,

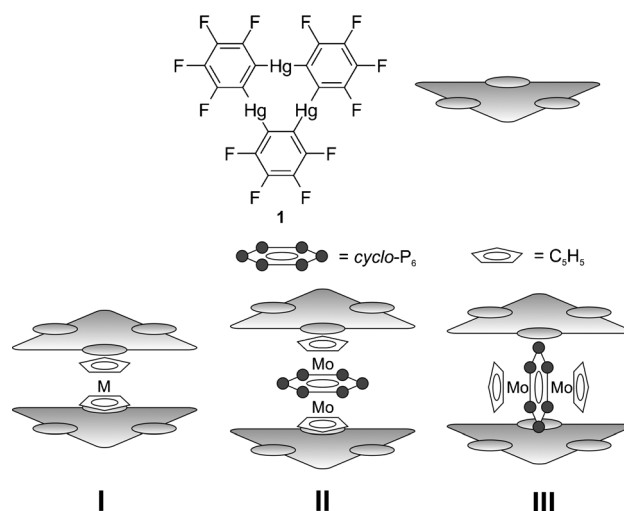
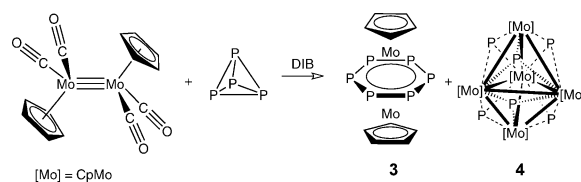


Figure 1. I) The double-sandwich structure that is obtained when reacting $[Cp_2Fe]$ or $[Cp_2Ni]$ with $[(o-C_6F_4Hg)_3]$. II) and III) Potential assemblies that would be expected to form in a reaction with a triple-decker sandwich complex containing a $cyclo-P_6$ middle deck.

we also wanted to determine whether the structure and formation of the adducts would be governed by $Cp \cdots Hg$ π interactions (type **II**) or hitherto unknown $P \cdots Hg$ interactions of **1** involving the P_6 middle deck (type **III**, Figure 1).

We first studied the reaction of $[(o-C_6F_4Hg)_3]$ (**1**) with the known triple-decker sandwich $[(Cp^*Mo)_2(\mu-\eta^6:\eta^6-P_6)]$ (**2**)^[8] in CH_2Cl_2 . According to ^{31}P and ^{19}F NMR spectroscopy, these two compounds do not interact in solution. This observation was corroborated by the crystallization of the individual components upon slow evaporation of the solvent. Realizing that the bulk of the Cp^* ligand might be responsible for this lack of interaction, we decided to investigate the synthesis of the Cp complex **3** in view of its interaction with **1** (Scheme 1). Inspired by our finding that compound **2** can be obtained in 64% yield by reaction of $[(Cp^*Mo(CO)_2)_2]$ with P_4 in



Scheme 1. Reaction of $[(CpMo(CO)_2)_2]$ with P_4 in 1,3-diisopropylbenzene.

[*] M. Fleischmann, C. Heindl, M. Seidl, Dr. G. Balázs, Prof. Dr. M. Scheer
Institut für Anorganische Chemie, Universität Regensburg
93040 Regensburg (Germany)
E-mail: manfred.scheer@chemie.uni-regensburg.de
Dr. A. V. Virovets, Dr. E. V. Peresyphkina
Nikolaev Institute of Inorganic Chemistry
Siberian Division of RAS
Acad. Lavrentyev prosp. 3, 630090 Novosibirsk (Russia)
M. Tsunoda, Dr. F. P. Gabbaï
Department of Chemistry, Texas A&M University
College Station, TX 77843 (USA)

[**] This work was supported by the Deutsche Forschungsgemeinschaft, the NSF (CHE-0952912), the Fonds der Chemischen Industrie, and the Alexander von Humboldt Foundation through the reinvitation program (F.P.G.). The COST action CM0802 PhoSciNet is gratefully acknowledged. We thank Prof. A. Y. Timoshkin for discussions concerning the DFT calculations.

Supporting information for this article (full synthetic and spectroscopic details for **3–6**, crystallographic details, and full details and references for the DFT calculations) is available on the WWW under <http://dx.doi.org/10.1002/anie.201204686>.

refluxing 1,3-diisopropylbenzene (DIB) rather than xylene, for which a yield of only 1% was reported,^[8] we allowed $[(\text{CpMo}(\text{CO})_2)_2]$ to react with P_4 at 205°C in DIB. Gratifyingly, this reaction afforded the expected compound $[(\text{CpMo})_2(\mu\text{-}\eta^6\text{:}\eta^6\text{-P}_6)]$ (**3**) as dark red crystals in an astonishing 12% yield (Scheme 1). The dark purple cluster $[(\text{CpMo})_5(\mu_3\text{-}\eta^1\text{:}\eta^1\text{:}\eta^1\text{-P})_6]$ (**4**) was also isolated as a side product of this reaction.^[9]

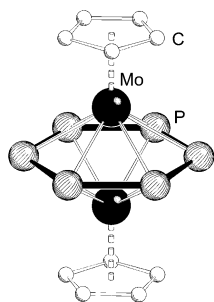


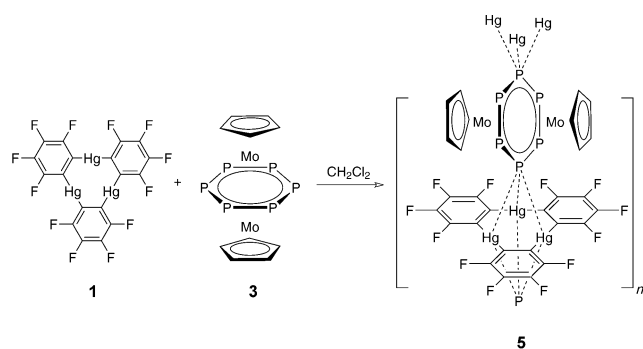
Figure 2. Molecular structure of **3**. H atoms are omitted for clarity.

The triple-decker sandwich complex **3** was characterized by single-crystal X-ray diffraction analysis (Figure 2). It consists of a planar *cyclo*- P_6 middle deck stabilized by CpMo fragments. All three rings are almost planar and parallel. The P–P distances are very similar, with an average length of 2.177(2) Å.

The triple-decker **3** shows a very low solubility in CH_2Cl_2 and THF when compared to its Cp^* analogue and no solubility in alkanes. The

^1H NMR spectrum of **3** in CDCl_3 shows a singlet at 2.54 ppm for the Cp protons, which represents a large upfield shift for the η^5 -bound Cp ring. This is induced by the anisotropy of the aromatic *cyclo*- P_6 ring, which was also observed for the methyl groups of Cp^* in compound **2**.^[8] In the ^{31}P NMR spectrum in CDCl_3 , only one singlet at –351.5 ppm is observed that is shifted to higher field, compared to **2** (–315 ppm).

With compound **3** in hand, we decided to attempt its assembly with **1** in CH_2Cl_2 (Scheme 2). While no adduct



Scheme 2. Formation of the one-dimensional stacking compounds **5**.

precipitation could be observed, slow diffusion of a layer of hexane into the reaction mixture resulted in the formation of orange crystals of the polymeric adduct $[\mathbf{1}\text{--}\mathbf{3}]_n$ (**5**). The ^{31}P NMR spectrum of **5** in CD_2Cl_2 shows a sharp singlet that is only shifted by 1.74 ppm when compared to that of pure **3**. This small shift as well as the absence of coupling to the ^{199}Hg nuclei suggests that the complex is extremely labile and exists mostly in a dissociated form in solution. In agreement with this conclusion, the field desorption mass spectrum of **5** only shows the peaks for the pure starting materials.

A systematic analysis of the single crystals obtained from this reaction indicates that polymeric **5** crystallizes with a varying number m of interstitial CH_2Cl_2 molecules, leading to $[\mathbf{5}\cdot(\text{CH}_2\text{Cl}_2)_m]_n$ ($1 \leq m \leq 2$; **5a–d**). All of these different solvates were obtained from solutions stored at –28°C, +4°C, and at room temperature, indicating that temperature cannot be used to selectively obtain a single solvate. Elemental analysis revealed that the interstitial CH_2Cl_2 molecules are completely removed upon drying in vacuum. Interestingly, recrystallization of **5** from a warm CH_2Cl_2 /hexane mixture results in the isolation of pure complex **3** along with a new adduct (**6**) as orange plates. Structural characterization of this new adduct indicated that it consists of discrete $[\mathbf{1}\text{--}\mathbf{3}\text{--}\mathbf{1}]$ supersandwiches with a molecule of **3** trapped between two molecules of **1**.

The crystal structures of **5a–d** indicate that the structure of the primary $[\mathbf{1}\text{--}\mathbf{3}]_n$ polymeric chain is not drastically affected by the varying number of interstitial CH_2Cl_2 molecules. In all cases, molecules of **1** and **3** alternate to form one-dimensional stacks (Figure 3a) that run parallel to each other

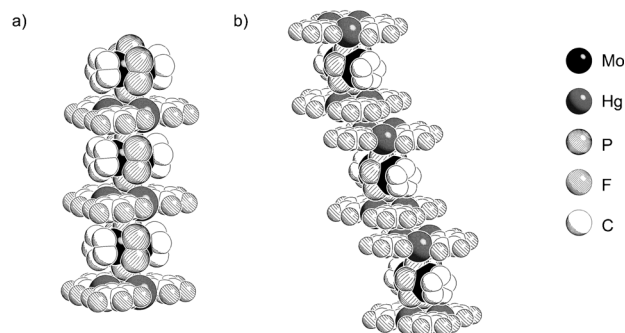


Figure 3. a) Representation of the crystal structure of **5a**, showing the one-dimensional polymeric stack. b) Crystal structure of **6**, showing the slanted stacks consisting of independent sandwich units. H atoms are omitted for clarity.

in the crystalline lattice. In each stack, the triple-decker complex **3** lies between two successive molecules of **1** with two opposite P atoms of the P_6 ring pointing towards the center of the closest Hg_3 triangle. Compound **6** on the other hand can be defined as a discrete supersandwich $[\mathbf{1}\text{--}\mathbf{3}\text{--}\mathbf{1}]$ complex in which opposite P atoms of the P_6 unit also point to the center of the closest Hg_3 triangle. In the crystal, these supersandwich units form slanted stacks which are shown in Figure 3b. The shortest observed intermolecular $\text{Hg}\cdots\text{Hg}$ distance for **6** is 3.5742(4) Å, which is slightly longer than 3.512 Å found for **1**-acetone^[10] or 3.564 Å found for pure **1**^[11] but significantly exceeds 3.3996 Å that is found for the double sandwich structure of **1** with $[\text{Cp}_2\text{Ni}]$ ^[7] and also 3.41 Å that was calculated for the dimer $[\text{HgMe}_2]_2$ ^[12] in the solid state.

Figure 4 shows a section of the crystal structure of **5a** as an example to explain the assembly of the compounds **5** and **6**. The phosphorus atoms P1 and P4 are located above the center of the three Hg atoms of molecule **1**, but the resulting P–Hg distances are not equivalent. There is a lively discussion in the

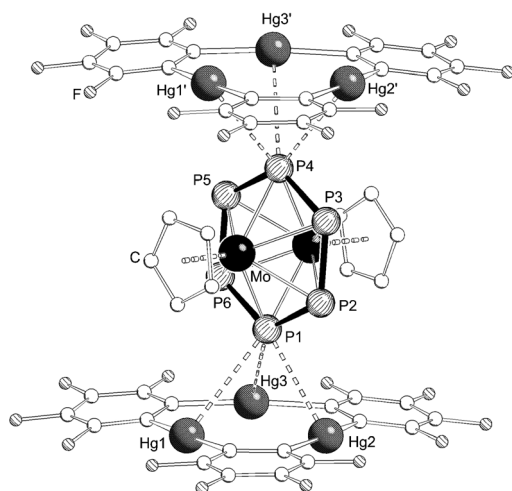


Figure 4. Section of the one-dimensional polymer in **5a**. H atoms are omitted for clarity.

literature^[12,13] about the van der Waals radius of mercury(II) in its different compounds, with reported values from 1.7 Å up to 2.2 Å. Table 1 compares the shortest P–Hg distance (sh. $d_{\text{Hg-P}}$), the average P–Hg distance ($\bar{\phi} d_{\text{Hg-P}}$), and also the average distance between the center of the three Hg atoms of

Table 1: Selected distances d [Å] and angles ϕ [°] of the different crystal phases of **5**.

	5a	5b	5c	5d
sh. $d_{\text{Hg-P}}$	3.195(3)	3.262(2)	3.295(2)	3.268(1)
$\bar{\phi} d_{\text{Hg-P}}$	3.340(3)	3.380(2)	3.328(2)	3.385(2)
$\bar{\phi} d_{\text{P-Z}}$	2.619(3)	2.643(2)	2.599(2)	2.676(2)
$\phi_{\text{Hg3-Hg3'}}$	0	17.77(2)	59.98(4)	18.61(2)
$\phi_{\text{P6-P6'}}$	0	70.20(3)	19.22(5)	70.30(2)

1 to the closest P atom ($\bar{\phi} d_{\text{P-Z}}$) that are found for each crystal structure **5a–d**. Even when taking the shortest value for the van der Waals radius of mercury (1.7 Å) into account, the observed P–Hg distances in **5a–d** are considerably shorter than the sum of the van der Waals radii for Hg and P (3.6 Å). These long P–Hg distances are consistent with very weak interactions and also exceed on average the intermolecular P–Hg distances (3.129(2) Å or 3.246(1) Å) found for the mercury(II) phosphido compounds $\text{Hg}(\text{PR}_2)_2$ ($\text{R} = t\text{Bu}$,^[14] SiMe_3 ^[15]) that form dimers in the solid state. The observed distances can be compared very well to the S–Hg distances found in $\mathbf{1} \cdot (\text{SMe}_2)_3$ ^[16] (3.24–3.47 Å).

The crystal structures **5a–d** show the biggest differences when looking at the arrangement of consecutive molecules of **1** or **3** along the stacking axis. The angles $\phi_{\text{Hg3-Hg3'}}$ and $\phi_{\text{P6-P6'}}$ (Table 1), describe the dihedral angle of either two consecutive molecules of **1** or **3**. It has to be noted, that since **1** shows a threefold symmetry in respect to the stacking direction, the maximum or minimum value for $\phi_{\text{Hg3-Hg3'}}$ is 0° and 60°, respectively, which would result in an eclipsed or staggered

arrangement of the three Hg atoms of **1** along the stack. The same consideration for **3** shows that the twofold symmetry with respect to the stacking axis results in a maximum value for $\phi_{\text{P6-P6'}}$ of 90°. This would describe a perpendicular arrangement of two consecutive P_6 rings. The notable variation observed in the $\phi_{\text{Hg3-Hg3'}}$ and $\phi_{\text{P6-P6'}}$ angles indicate that rotation of the unit along the stacking direction may be facile, leading to structures of similar energy.

DFT calculations^[17] on the experimentally observed geometry of **6** shows that the phosphorus atoms possess a lone pair of electrons each. Those of P1 and P4 (see Figure 4) are directed toward the middle of the Hg_3 triangle (Figure 5). This arrangement suggests that an orbital inter-

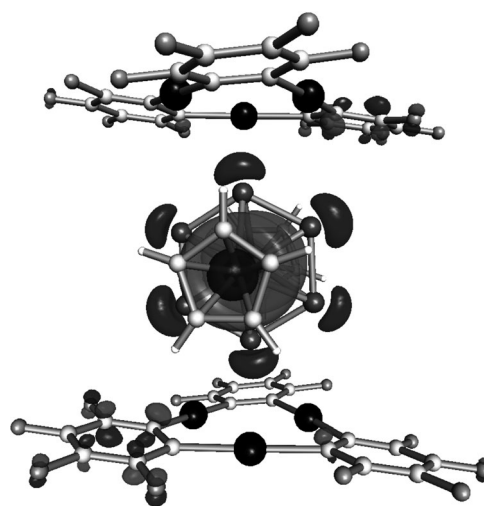


Figure 5. a) Isosurface of the HOMO-2 in **6** representing the Mo–Mo bond as well as the contribution of the phosphorus lone pairs.

action with a corresponding acceptor orbital (that is, the LUMO of **1**^[18] containing atomic orbital contributions from Hg) is possible, at least from a geometric point of view. However, the calculations show that the electronic structure of **6** is approximately the superimposition of the electronic structure of the separated fragments.

In summary, we have presented the synthesis of the hitherto unknown triple-decker complex $[(\text{CpMo})_2(\mu\text{-}\eta^6\text{-}\eta^6\text{-P}_6)]$ (**3**) whose formation is accompanied by that of the novel paramagnetic cluster $[(\text{CpMo})_5(\mu_3\text{-}\eta^1\text{-}\eta^1\text{-}\eta^1\text{-P})_6]$ (**4**). Mixing **3** with the trinuclear mercury complex **1** in CH_2Cl_2 results in the formation of adducts with polymeric (**5**) or discrete super-sandwich structures (**6**). A common feature of these adducts is the observed perpendicular intercalation of a molecule of **3** between two molecules of **1**. This unique arrangement is supported by multiple $\text{P} \cdots \text{Hg}$ interactions that are shorter than the sum of the van der Waals radii and that involve opposite atoms of the P_6 units and the three mercury atoms of the Hg_3 complex. Although the coordination chemistry of **1** has been widely investigated, adducts with direct $\text{P} \cdots \text{Hg}$ interactions had never been observed prior to this work. We also note that despite their noted weakness, the formation of $\text{P} \cdots \text{Hg}$ interactions is definitely favored over that of $\text{Hg} \cdots \text{Cp}$

π interactions that have been observed in the ferrocene and nickelocene adducts of **1**.^[7]

Received: June 15, 2012

Revised: July 16, 2012

Published online: September 3, 2012

Keywords: mercury · phosphorus · polymers · weak interactions · π - π stacking

- [1] J. W. Steed, J. L. Atwood, *Supramolecular Chemistry*, 2nd ed. Wiley, Weinheim, **2009**.
- [2] a) B. L. Schottel, H. T. Chifotides, K. R. Dunbar, *Chem. Soc. Rev.* **2008**, 37, 68–83; b) B. P. Hay, V. S. Bryantsev, *Chem. Commun.* **2008**, 2417–2428; c) A. Frontera, P. Gamez, M. Mascal, T. J. Mooibroek, J. Reedijk, *Angew. Chem. Int. Ed.* **2011**, 50, 9564–9583.
- [3] J. F. Stoddart, *Chem. Soc. Rev.* **2009**, 38, 1802–1820.
- [4] a) M. R. Haneline, R. E. Taylor, F. P. Gabbaï, *Chem. Eur. J.* **2003**, 9, 5189–5193; b) T. J. Taylor, C. N. Burress, F. P. Gabbaï, *Organometallics* **2007**, 26, 5252–5263.
- [5] a) P. Sartori, A. Golloch, *Chem. Ber.* **1968**, 101, 2004–2009; b) A. S. Filatov, E. A. Jackson, L. T. Scott, M. A. Petrukhina, *Angew. Chem.* **2009**, 121, 8625–8628; *Angew. Chem. Int. Ed.* **2009**, 48, 8473–8476; c) V. B. Shur, I. A. Tikhonova, *Russ. Chem. Bull.* **2003**, 52, 2539–2554.
- [6] a) C. N. Burress, M. I. Bodine, O. Elbjeirami, J. H. Reibenspies, M. A. Omary, F. P. Gabbaï, *Inorg. Chem.* **2007**, 46, 1388–1395; b) M. R. Haneline, J. B. King, F. P. Gabbaï, *Dalton Trans.* **2003**, 2686–2690; c) M. R. Haneline, M. Tsunoda, F. P. Gabbaï, *J. Am. Chem. Soc.* **2002**, 124, 3737–3742; d) M. Tsunoda, F. P. Gabbaï, *J. Am. Chem. Soc.* **2000**, 122, 8335–8336; e) I. A. Tikhonova, D. A. Gribanyov, K. I. Tugashov, F. M. Dolgushin, A. S. Peregodov, D. Y. Antonov, V. I. Rosenberg, V. B. Shur, *J. Organomet. Chem.* **2010**, 695, 1949–1952.
- [7] M. R. Haneline, F. P. Gabbaï, *Angew. Chem.* **2004**, 116, 5587–5590; *Angew. Chem. Int. Ed.* **2004**, 43, 5471–5474.
- [8] O. J. Scherer, H. Sitzmann, G. Wolmershäuser, *Angew. Chem.* **1985**, 97, 358–359; *Angew. Chem. Int. Ed. Engl.* **1985**, 24, 351–353.
- [9] The crystal structure of **4** is presented in the Supporting Information.
- [10] J. B. King, M. R. Haneline, M. Tsunoda, F. P. Gabbaï, *J. Am. Chem. Soc.* **2002**, 124, 9350–9351.
- [11] M. R. Haneline, F. P. Gabbaï, *Z. Naturforsch. B* **2004**, 59, 1483–1487.
- [12] P. Pyykkö, M. Straka, *Phys. Chem. Chem. Phys.* **2000**, 2, 2489–2493.
- [13] a) J. S. Casas, M. S. Garcia-Tasende, J. Sordo, *Coord. Chem. Rev.* **1999**, 193–195, 283–359; b) S. S. Batsanov, *J. Chem. Soc. Dalton Trans.* **1998**, 1541–1546; c) K. R. Flower, V. J. Howard, S. Naguthney, R. G. Pritchard, J. E. Warren, A. T. McGown, *Inorg. Chem.* **2002**, 41, 1907–1912; d) A. J. Canty, G. B. Deacon, *Inorg. Chim. Acta* **1980**, 45, L225–L227.
- [14] S. Scholz, M. Bolte, M. Wagner, H.-W. Lerner, *Z. Anorg. Allg. Chem.* **2007**, 633, 1199–1204.
- [15] S. C. Goel, M. Y. Chiang, D. J. Rauscher, W. E. Buhro, *J. Am. Chem. Soc.* **1993**, 115, 160–169.
- [16] M. Tsunoda, F. P. Gabbaï, *J. Am. Chem. Soc.* **2003**, 125, 10492–10493.
- [17] For details, see the Supporting Information.
- [18] M. R. Haneline, F. P. Gabbaï, *Inorg. Chem.* **2005**, 44, 6248–6255.